

# Study of the Impact of Droplets on Superhydrophobic Surfaces

Rongxian Zhu, Ting Chen, Shanshan Luo, Kaiyuan Yang\*

School of Art and Design, Suzhou Centennial College, Suzhou 215000, Jiangsu Province, China

\*Corresponding author: Kaiyuan Yang, kaiyuan689@gmail.com

**Copyright:** © 2024 Author(s). This is an open-access article distributed under the terms of the Creative Commons Attribution License (CC BY 4.0), permitting distribution and reproduction in any medium, provided the original work is cited.

**Abstract:** The potential applications of superhydrophobicity for self-cleaning, microfluidic systems, and so on, inspired by the “lotus leaf effect”, have recently attracted great attention from academia and industry. To date, however, neither experimental nor theoretical studies have reached the scalable application of superhydrophobic surfaces, and no simple methods have been developed to produce durable superhydrophobic surfaces. In this project, conical, cylindrical, and cube microstructures with different shapes and dimensions were prepared by 3D printing. Among these structures, the conical microstructures without further modification exhibited the best hydrophobic performance with a contact angle of 120°. However, the hydrophobic performance of the cube microstructures was significantly improved with the addition of an FAS coating to the surface, reaching 131°. This indicates that, with the help of the coating, the 3D printed materials with special features can be transformed into hydrophobic surfaces. The outcome of this project will be useful in promoting the efficient and low-cost preparation of superhydrophobic functional surfaces and their engineering applications.

**Keywords:** 3D printing; Superhydrophobicity; Contact angle; Hysteresis; Microstructure

**Online publication:** September 27, 2024

## 1. Introduction

### 1.1. Introduction to material surfaces and interfaces

In general, the wettability of a solid material surface depends mainly on the chemical composition of the surface and the microscopic surface morphology. Under certain conditions, changes in environmental factors (temperature or pressure) can also significantly alter wettability. Research and development of materials with specific surface wettability is therefore important to deepen the understanding of physical and chemical phenomena on surfaces, to broaden the range of applications, and to improve material properties. The surface point of action of a material influences the general properties of the material <sup>[2]</sup>.

Nature has provided the material basis for the development of bionanotechnology. The most representative of nature is the superhydrophobic phenomenon of the lotus leaf. The lotus leaf has attracted a great deal of

attention from science and industry for its self-cleaning properties. Water droplets on a lotus leaf (contact angle  $161.0 \pm 2.7^\circ$ , roll angle only  $2^\circ$ ) roll freely and carry contaminants away from the surface, showing us the amazing superhydrophobic self-cleaning phenomenon in nature (also known as the “lotus leaf effect”) [3]. In addition to the lotus leaf, many other organisms have similar hydrophobic properties. Superhydrophobic surfaces are academically rigorously defined as unique surfaces with great applications based on the static and dynamic characteristics of water droplets [12]. The wetting state of a solid surface by water is usually described by two parameters: the static apparent contact angle and the contact angle hysteresis. The angle  $\theta$  between the tangent to the gas-liquid interface at the point of intersection of the gas, liquid, and solid phases and the solid-liquid partition line across the three-phase contact point is the contact angle of the liquid on the solid surface [5].

## 1.2. Aim and objective

The study of hydrophilicity in nature has led to various theories and methods for the preparation of superhydrophobic surfaces. However, there are still several problems to be solved in the study of the preparation and wetting mechanisms of superhydrophobic functional surfaces. Amongst these are the common disadvantages of existing preparation methods such as low efficiency, long time, and high cost. Therefore, the development of efficient, low-cost, and environmentally friendly preparation techniques, the elucidation of the wetting mechanism of surfaces, the study of the quantitative relationship between the geometry of surface structures and surface wettability, and the improvement of their controllability, strength, and durability have become hot spots in the study of superhydrophobic functional surfaces.

Based on this, this project combines CAD modeling and 3D printing techniques to prepare superhydrophobic functional surfaces to obtain array samples with different shapes and feature sizes. It is expected to improve the preparation efficiency of superhydrophobic functional surfaces, reduce cost, improve droplet anisotropy controllability, and obtain an array of structure types and parameters with desirable superhydrophobic properties. Hopefully, this research will be of scientific significance and engineering value in promoting the efficient and low-cost preparation of superhydrophobic functional surfaces and their engineering applications.

## 2. Literature review

### 2.1. Theoretical models of superhydrophobic wettability

As early as 1805, the British physicist Thomas Young proposed the famous Young equation for an ideal rigid, smooth surface, which laid the theoretical foundation for studying the wetting behavior of solid surfaces [12]. When a water droplet is stationary on a solid surface, the static contact angle between the droplet and the solid surface results from the interaction of surface tensions at the solid, liquid, and gas interfaces. Based on the mechanical equilibrium conditions, in the horizontal direction, Young obtained the following equation for droplet equilibrium [13]. However, Young’s model did not consider the existence of rough structures. For this reason, in 1936, Wenzel revised Young’s equation and introduced the concept of the “Roughness factor” [15]. However, Cassie and Baxter found that Wenzel’s equation was not applicable when the solid surface consisted of different types of chemicals [1]. The concept of “composite contact” was introduced, and a new model, the Cassie model (**Figure 1**), was developed to describe the composite infiltration state. Since then, Jopp et al. have carefully investigated those changes in the rough structure of a solid surface can also lead to a shift in the wetting state between the Wenzel and Cassie models [7].

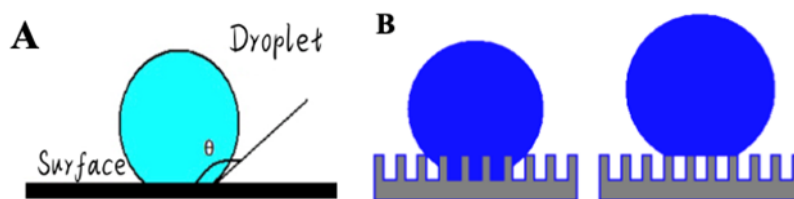


**Figure 1.** A) Contact angle; B) Wenzel Model and Cassie-Baxter Model

## 2.2. Factors affecting the properties of superhydrophobic surfaces

SEM and ESEM observations and performance tests of superhydrophobic surfaces have shown that superhydrophobicity is mainly determined by the physical structure and chemical composition of the surface<sup>[1]</sup>. Experimental observations and theoretical studies have shown that micromorphology influences the hydrophobic properties of a surface and the stability of the surface structure (**Figure 2**). Only a suitable surface microgeometry can constitute a stable superhydrophobic surface<sup>[17]</sup>. This secondary hierarchy leads to superhydrophilicity<sup>[4]</sup>. By modeling the thermodynamic geometry of superhydrophobic surfaces, Li and Amirfazli analyzed the influence of the physical structure of solid surfaces on superhydrophobic properties<sup>[9-10]</sup>. The contact angle hysteresis of different surfaces at the micro and nano roughness fractal level was obtained by calculating the free energy and energy barriers of surfaces at different roughness scales.

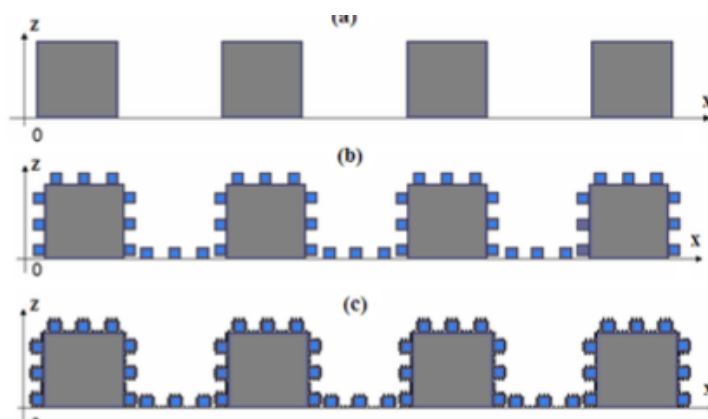


**Figure 2.** Schematic representation of the surface multilevel rough microstructure<sup>[11]</sup>

## 2.3. Biomimetic preparation of superhydrophobic surfaces

Micromorphology is a key factor influencing droplet wetting on solid surfaces and therefore superhydrophobic surfaces can be prepared by modifying low surface energy materials on rough surfaces with micro- and nano-morphologies or by constructing micro- and nano-scale morphologies on the surface of hydrophobic materials<sup>[9]</sup>. However, the high complexity of the preparation process, the low durability, and the severe environmental pollution caused by the preparation process are problems to be faced.

Despite its prevalence in microelectronics and medical-biological fields, lithography has certain limitations. As a result, while conventional lithography has been used to push the “limits” of resolution, other techniques such as electron beam lithography, X-ray lithography, and nanoimprinting have also been investigated<sup>[8]</sup>. Over the past few years, lithography has been used extensively to create hydrophobic, self-cleaning surfaces.

Electrochemical deposition is broadly utilized in the planning of bionic superhydrophobic surfaces. Wang et

al. used a simple electrochemical deposition method to prepare copper mesh films with micro/nanostructures [13]. After its modification using long-chain fatty acids, the structure shows that the layered structure of the copper film and the nature of the long-chain fatty acids work together to produce a superhydrophobic, superlipophilic surface. Zheng et al. obtained new chromate chemically transformed films with superhydrophobic and self-healing properties by depositing a deep eutectic solvent containing Cr(III) on the surface of magnesium alloys modified with stearic acid [16]. The advantage of this method is that trivalent chromium is less toxic and less polluting to the environment than hexavalent chromium in conventional schemes.

Compared with other methods, laser etching is characterized by fast cutting speed and high accuracy, and can obtain stable three-dimensional layered structures and regular superhydrophobic arrays, thus solving the problem of uneven distribution of rough structures on superhydrophobic surfaces [6]. In addition, laser etching can be used to obtain transparent superhydrophobic surfaces. The high cost combined with the long preparation period would limit the economics of any practical application to large-scale use.

The process of forming superhydrophobic micro and nano surface structures by 3D printing technology is highly like the natural formation process of biological materials, which can simultaneously control the material's local chemical composition and fine structure, enabling the preparation of highly complex and functional materials with excellent performance. Wei et al. used 3D printing technology with low surface energy modification to produce superhydrophobic microporous membranes for oil-water separation to solve the problem of oil spill pollution caused by the development of the oil industry [14]. It is easy and cheap to prepare. It is also possible to achieve a high degree of precision and complexity in the physical product, allowing for the manufacture of very complex parts that are not possible with traditional methods.

In summary, research in the field was reviewed and the advantages and disadvantages of some preparation methods were compared (Figure 3). As a result, it was found that 3D printing is a technique capable of preparing a model of a microsurface structure in a short time. Although it can face the problem of low structural accuracy, it is a good option for short-term projects with the advantages of a simple preparation process, low preparation costs, and high material utilization.

Comparison of superhydrophobic surface preparation methods			
Method	Process	Advantages	Disadvantages
lithography	The pattern is drawn onto a flat stone (or a prepared metal plate, usually zinc or aluminium) and adhered by means of a chemical reaction.	High resolution, Ability to obtain good models of results, easy to handle.	High cost, decreases sensitivity in equal proportion as resolution increases.
Electrochemical deposition	Plating is formed by the migration of positive and negative ions through the electrolyte solution under the influence of an external electric field and the redox reaction of gaining and losing electrons at the electrode.	Simple process, low cost, high efficiency and easy to control.	Environmental pollution problems, poor coating strength and wear resistance.
Laser etching	Laser ablation of the surface to change the rough structure of the surface.	Precise control of parameters, good surface stability	High cost and long cooling time.
3D printing	It is a rapid formation technique that uses a digital model file as a basis for constructing objects by layer-by-layer build-up of bondable materials.	High material utilisation, simple preparation process and low preparation costs.	High machine input costs and material limitations.
Chemical deposition	Is formed by the reaction between the substrate and a solution or gas containing a metal element.	Time saving, low cost	Poor abrasion resistance, can pollute the environment and is also difficult to control

**Figure 3.** Comparison of superhydrophobic surface preparation methods

### 3. Research methodologies

The research objectives of this project are to improve the efficiency of the preparation of superhydrophobic functional surfaces, to reduce costs, to improve the controllability of droplet anisotropy, and to obtain a range of structure types and parameters with desirable superhydrophobic properties. A combination of theoretical analysis and experimental studies was used in this project. Firstly, from the point of view of data collection and analysis methods, an analytical approach of qualitative analysis was initially adopted in the literature review section. The basis for research and analysis of the core themes was laid down primarily through the reading and summarization of academic papers. Recent research on the theory of superhydrophobicity and superhydrophobic phenomena in nature is presented and analyzed, and methods of preparing superhydrophobic surfaces and their applications are outlined, and the advantages and disadvantages of each preparation method are summarized. Theoretical studies and experimental structures are complementary, and the design of subsequent experimental models and preparation methods are laid down through preliminary theoretical studies (**Figure 4**).

All data used in the thesis were derived from real measurements in the school laboratory. The experimental data used in the results were averaged and calculated using a formula after 5 measurements to produce the data in the table.

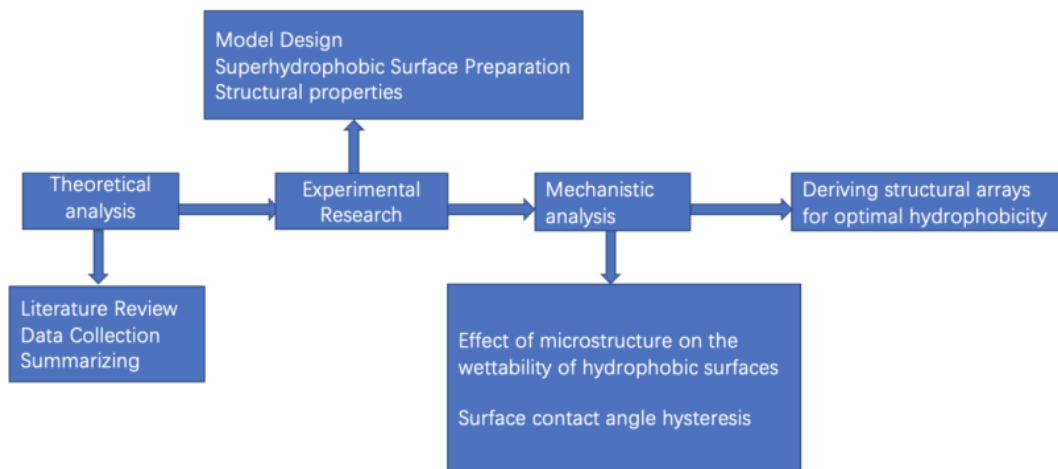


**Figure 4.** Project research route map

### 3.1. Experimental methods

#### 3.1.1. Design of the surface structure

A simple columnar model was first designed in Auto CAD drawing software to simulate the superhydrophobic surface, inspired by the first-level columnar microstructure morphology of the cicada and silicon wafer surfaces. The style of the microstructure has also been changed, with the addition of models with different dimensions, shapes, feature sizes, cylinders, and flat shapes (**Figure 5**). All the above models are based on changing the geometrical parameters and shapes of the microstructure, thus controlling the critical contact angle and the wetting behavior in different states.

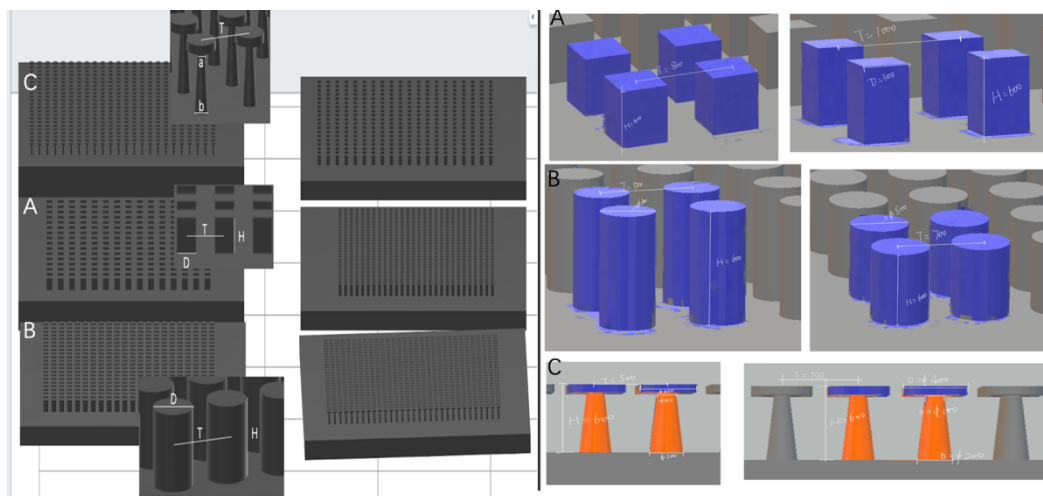


**Figure 5.** Dimensions of key models. A) Pillar model group (Key geometrical parameters: D, T, and H are the diameter, spacing (center-to-center), and height of the micropillar, respectively. Parameters on the left are  $D = 500 \mu\text{m}$ ,  $T = 800 \mu\text{m}$ , and  $H = 600 \mu\text{m}$  respectively. B) Cylindrical model group and Flat model group. The key geometrical parameters: D, T, and H are the diameters, spacing (center to center), and height of the micropillar respectively. The parameters on the left are  $D = 300 \mu\text{m}$ ,  $T = 500 \mu\text{m}$  and  $H = 600 \mu\text{m}$  respectively; On the right are  $D = 500 \mu\text{m}$ ,  $T = 700 \mu\text{m}$ , and  $H = 600 \mu\text{m}$  respectively. C) Flat model group Key geometric parameters: D, T, and H are the diameter, spacing (center to center), and height of the micropillar respectively. a and b are the diameter of the top end and the diameter of the bottom surface of the cylinder. The parameters on the left are  $D = 400 \mu\text{m}$ ,  $T = 500 \mu\text{m}$ ,  $H = 600 \mu\text{m}$ ,  $a = 100 \mu\text{m}$  and  $b = 200 \mu\text{m}$ . The parameters on the right are  $D = 400 \mu\text{m}$ ,  $T = 700 \mu\text{m}$ ,  $H = 600 \mu\text{m}$ ,  $a = 100 \mu\text{m}$  and  $b = 200 \mu\text{m}$ .

### 3.1.2. Measurement of contact angles

To further characterize the wettability of the surface, static contact angles, forward contact angles, as well as backward contact angles, were measured on nine existing samples and seven samples of the new design.

The contact angles were measured using a DataPhysics OCA20 goniometer. The contact angle measurement instrument consists of five main components: the light source, the injection unit, the sample stage, the acquisition system, and the analysis software. The device uses the principle of optical imaging. The static drop method is used. A drop of liquid is placed on the solid surface, the equilibration system is photographed after equilibration at the solid-liquid-gas three-phase interface and the contact angle is measured using the contact angle measurement method provided by the software. The equilibration process can also be photographed or videoed at regular intervals during the test. In the sessile droplet mode, the measurement is controlled by controlling the volume of the injected droplet and the injection rate entered in the injection volume, and by adjusting the position of the two reference lines. The exact angle can then be obtained by automatically or manually positioning the shape of the droplet.

### 3.1.3. Measuring the ACA and the RCA

The reason for estimating the dynamic contact points is to characterize the hydrophobic properties of the 3D printed material. Measuring ACA and RCA is also done using a DataPhysics OCA20 Goniometer. ACA and RCA points are obtained using ARCA estimation strategies. As shown in the diagram, the results graph takes the form of a curve. When the curve shows a straight line drop and the drop to the lowest point shows a steady

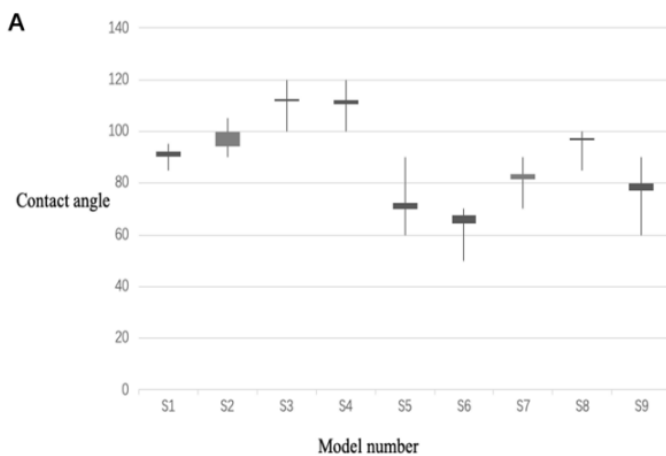
state, select this smooth section of the line, and the average value of the RCA is automatically calculated in the results box. Similarly, when the curve rises in a straight line from a steady state, a numerical line of ACA appears, which is manually selected and the average value is automatically calculated. This task is repeated six times and finally, all the data is combined and the respective average values of ACA and RCA are calculated. Multiple measurements are taken to reduce errors in the final experimental data. The accuracy of the experiment is ensured.

## 4. Results and analysis

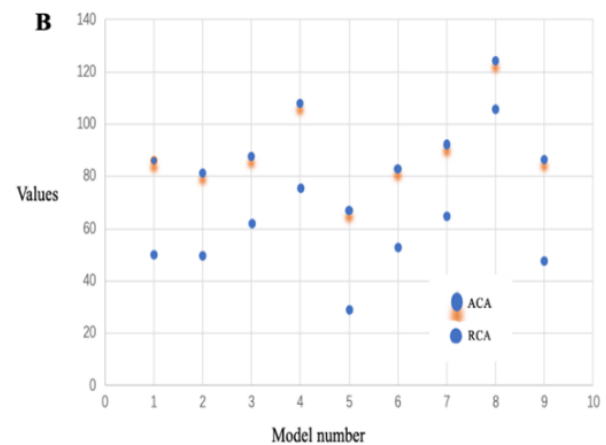
### 4.1. Experiment 1

Nine existing models were used for this experiment, and this set of models were all cylindrical arrays. The basic data for these models were set up with height as the quantitative and width and spacing as the variable. This experiment observed the CA, ACA, and RCA of the modified group of models. The results of the experiment were tabulated. Based on **Figure 6**, S1–S9 were rearranged according to the diameter dimensions of the surface structures. As can be seen from the figure, with the same microsurface diameter, the smaller the distance between the surface micropillars, the larger the contact area of the water droplet (5  $\mu\text{l}$ ) on the surface micropillars, and therefore the droplet is less likely to come into contact with the model surface and its surface is less wettable. Conversely, the greater the distance between the microcolumns, the smaller the contact area of the water droplets on the surface microcolumns and the easier it is for the droplets to wet the surface of the model, when the model is more hydrophilic. The present experimental data shows that the model's best hydrophobic performance is achieved when the height of the surface micropillar is constant,  $D = 4$  mm and  $T = 3$  mm. The static contact angle reaches  $112.18^\circ$ , which is greater than  $90^\circ$ , so the model achieves hydrophobic performance.

The contact angle satisfies the Young equation on an ideal surface that is smooth, chemically homogeneous, rigid, and free from interactions such as chemical reactions. The contact angle on a real surface is not unique as predicted by the Young equation but varies between two relatively constant angles, a phenomenon known as contact angle hysteresis. As can be seen in **Figure 6**, the relationship between roughness and wetting hysteresis is not monotonic but decreases with increasing roughness in the hydrophilic state.



**A:** Contact angle data for S1-S9.



**B:** ACA and RCA data for S1-S9.

Figure 6. Experiment 1 results overview table

## 4.2. Experiment 2

The samples involved in this experiment are newly designed samples of different shapes from this paper. There are seven samples printed by the 3D printer Formlab 3B. This set of samples was divided into three groups of different shapes and a model was damaged due to incomplete printing. As can be seen in **Figure 6**, the contact angle of the Flat 1 model has reached  $120.51^\circ$  in the surface contact angle measurement data. The inset shows a  $5\ \mu\text{l}$  droplet deposited on a surface like a micro-pillar. The illustration shows that in S5 in its uncoated state, the droplet has taken on a Cassie state on that surface.

According to the data shown in **Figure 7**, the larger the microstructure surface and the greater the contact angle between the droplet and the microstructure surface, the better the surface's hydrophobic properties when the height of the microstructure and the spacing between two adjacent microcolumns are the same (**Figure 8**). As can be seen in the third column of **Figure 7**, a control group was added to the same measurement experiment. This group had a chemical coating on the surface (FAS coating). For each type of microcolumn, five replicate measurements were performed on six separate microcolumns to verify accuracy and reproducibility. As can be seen from the data, the contact angle between all droplets and the surface is greater than  $110^\circ$  when covered with the coating, with an optimum of  $131.64^\circ$ . They are also measured mostly in the Cassie state, where the Wenzel Model is also present. Also, we can see from **Figure 7** that Pillar 1&2, and Flat 2 show a significant increase in the hydrophobicity of the models with the addition of the coating, by  $23\text{-}28^\circ$ . Conversely, the data obtained with and without the coating are not significant in the remaining three models. In particular, the Cylinder-looking microstructure, with or without coating, shows a hydrophobic state with a contact angle of  $110 \pm 10^\circ$ .

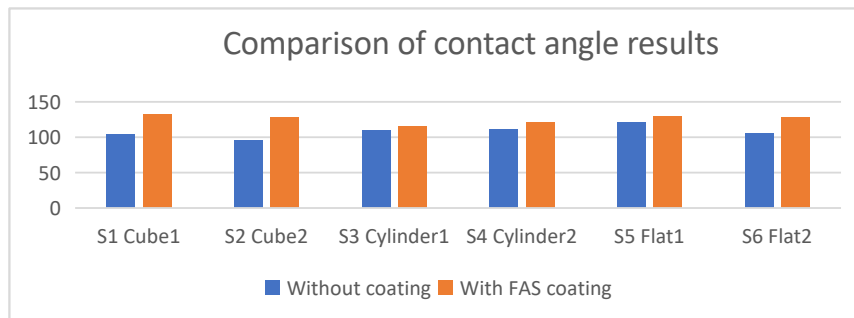
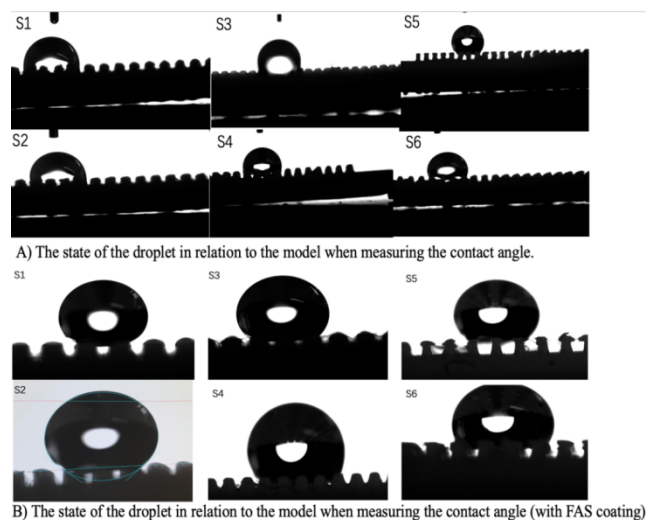


Figure 7. Experiment 2 results overview





**Figure 8.** The state of the droplet about the model when measuring the contact angle

### 4.3 Analysis

All data from experiments 1 and 2 were combined and analyzed. Firstly, the hydrophobicity of surfaces with different microforms was compared. As artificial superhydrophobic surfaces, one would expect the best dynamic properties. Secondly, the hydrophobicity of surfaces with different micromorphologies was analyzed in the wetted state. Within the range of conventional morphologies discussed, surfaces with a circular flat-shaped micromorph were found to have better hydrophobicity, followed by cylindrical and cube shapes. However, due to the limited accuracy of the models prepared by the 3D instruments used in this project, in most cases, the appearance presented by the goniometer was mostly cylindrical, and only minor variations would exist.

Comparison of contact angles between surfaces with a single microstructure and surfaces covered with FAS. The comparison shows that the contact angle increases significantly from  $94.6^\circ$  to  $128.3^\circ$  due to the coating compound. Furthermore, when measuring the contact angle of a single microstructured surface, a transition from the Cassie state to the lower contact angle Wenzel state occurs when the droplet wets the surface due to some kind of disturbance (dropping or shaking). A and B in **Figure 8** show the state of the droplet on the nanostructure, corresponding to the results in **Figure 7**. It can be seen from the figures that when the droplet meets the surface of a single microstructure, it will in most cases exhibit the Wenzel state. It is shown in **Figure 8B** that the droplet gets transformed on the model when a second layer of microstructure is added to the single microsurface. The state of the microsurface model for the cube shape gets significantly altered from the Wenzel state to the Cassie state. The state of the model for the flat shape is relatively stable and does not change significantly with the addition of the coating, remaining in the Cassie state. The microsurface structure of the cylinder, on the other hand, has not been greatly improved. Although the data in **Figure 7** shows that this surface is already hydrophobic, when the droplets still penetrate through the microcolumn to the surface, they present a Wenzel state. It can be seen that the droplet is most stable on the surface of the model when the structure of the microcolumn on the microsurface is flat (**Figure 7 S5**). The microsurface structure with a cube shape, on the other hand, is the structural surface that is most improved with the help of the coating.

### 4.4. Limitations

During the conduct of the experiments in this project, several limitations were encountered which resulted in inaccuracy. Firstly, unfortunately, the various dimensions of the existing models used in Experiment 1 were only estimated likely with errors. The second is that when using the OCA20 goniometer to measure CA, ACA, and RCA, the contact angle measurements from the goniometer are inherently inaccurate due to errors in the precise positioning of the reference line and the commissioning of the optics. As a result, they all have to be measured multiple times to minimize the generation of errors. Secondly, the models used in this project were all prepared by 3D printing technology. As the innate framing standards and improvement of 3D printing innovation are not yet great, the precision (counting layered exactness, shape exactness, and surface unpleasantness) and actual properties (like strength, firmness, weakness obstruction, and so on) of the printed parts are dependent upon specific limitations and don't recreate the shapes on the plan drawings well. As a result, the experimental results are not sufficiently satisfactory. Nevertheless, the experimental data so far show that the reformulated model also achieves a good hydrophobic state.

## 5. Conclusion

In summary, this project was rapidly modeled using Auto CAD and printed using a 3D printer. The models used were divided into two groups, where again by attaching FAS coatings to the surface of nanopillars on top of micro-pillars of different shapes. The contact angle is inversely proportional to the roughness up to an apparent contact angle of  $90^\circ$ . This means that as the roughness increases, the contact angle decreases, making it more hydrophilic. The behavior of hydrophobic surfaces is the opposite: as roughness increases, the contact angle increases. In the range of conventional forms discussed, the relationship between surface roughness and wettability is not monotonic but decreases with increasing roughness in the hydrophilic state, when the microstructure surface shapes (all cylindrical) are the same. When the basic dimensions of the microstructures were identical, the platform-shaped microstructure surfaces were found to be better hydrophobic, followed by the cylindrical and square shapes, which reached an original contact angle of  $120.51^\circ$ . In particular, the cylindrical-appearing microstructures, with or without coating, exhibited a hydrophobic state with a contact angle of  $110 \pm 10$ . However, the square microstructure surfaces with a two-layer structure had better hydrophobic properties, with the contact angle between the droplet and the model reaching  $131.54^\circ$ .

The 3D printer used in this project has huge limitations in terms of the size of the model and the accuracy is not optimal. However, 3D printing technology is certainly the best option for models that need to be prepared in a short period with different array structures. 3D printing can create new models for experiments in a short period. In any case, 3D printing technology has been a very popular technology in recent years and is being referenced by many industries for a wide range of applications. With the continuous development of 3D printing technology, its technical complexity and technical cost are constantly decreasing, which makes it possible to prepare superhydrophobic surfaces with micro and nano morphological structures in large areas and at low cost.

## Disclosure statement

The authors declare no conflict of interest.

## References

- [1] Cassie ABD, Baxter S, 1944, Wettability of Porous Surfaces. *Transactions of the Faraday Society*, 1944(40): 546–551.
- [2] Celia E, Darmanin T, Givenchy ETD, et al., 2013, Recent Advances in Designing Superhydrophobic Surfaces. *Journal of Colloid and Interface Science*, 2013(402): 1–18.
- [3] Feng C, Zhang W, Deng C, et al., 2017, 3D Printing of Lotus Root-like Biomimetic Materials for Cell Delivery and Tissue Regeneration. *Advanced Science*, 4(12): 1700401.
- [4] Feng L, Li S, Li Y, et al., 2002, Super-hydrophobic Surfaces: From Natural to Artificial. *Advanced Materials*, 14(24): 1857–1860.
- [5] Gu T, Zhu B, Ma J, 2001, *Surface Chemistry*. Science Press, Beijing.
- [6] Jagdheesh R, Garcia-Ballesteros JJ, Ocana JL, 2016, One-step Fabrication of Near Superhydrophobic Aluminum Surface by Nanosecond Laser Ablation. *Applied Surface Science*, 2016(374): 2–11.
- [7] Jopp J, Grull H, Yerushalmi-Rozen R, 2004, Wetting Behavior of Water Droplets on Hydrophobic Microtextures of Comparable Size. *Langmuir*, 20(23): 10015–10019.
- [8] Lawson RA, Robinson AP, 2016, Overview of Materials and Processes for Lithography. *Frontiers of*

Nanoscience, 2016(11): 1–90.

- [9] Li W, Ma XJ, Xu JL, et al., 2021, Effects of Base Angle and Wettability of Nanostructures on Droplet Wetting Behaviors. *Acta Physica Sinica*, 2021(70): 126101.
- [10] Liu HH, Zhang HY, Li W, 2011, Thermodynamic Analysis on the Wetting Behavior of Hierarchical Structured Superhydrophobic Surfaces. *Langmuir*, 27(10): 6260–6267.
- [11] Li W, Amirfazli A, 2008, Hierarchical Structures for Natural Superhydrophobic Surfaces. *Soft Matter*, 4(3): 462–466.
- [12] Young T, 1805, An Essay on the Cohesion of Fluids. *Philosophical Transactions of the Royal Society of London*, 1805(95): 65–87.
- [13] Wang S, Li Y, Fei X, et al., 2011, Preparation of a Durable Superhydrophobic Membrane by Electrospinning Poly (vinylidene fluoride)(PVDF) Mixed with Epoxy–siloxane Modified SiO<sub>2</sub> Nanoparticles: A Possible Route to Superhydrophobic Surfaces with Low Water Sliding Angle and High Water Contact Angle. *Journal of Colloid and Interface Science*, 359(2): 380–388.
- [14] Wei Q, Wang Y, Chai W, et al., 2017, Molecular Dynamics Simulation and Experimental Study of the Bonding Properties of Polymer Binders in 3D Powder Printed Hydroxyapatite Bioceramic Bone Scaffolds. *Ceramics International*, 43(16): 13702–13709.
- [15] Wenzel RN, 1936, Resistance of Solid Surfaces to Wetting by Water. *Industrial & Engineering Chemistry*, 28(8): 988–994.
- [16] Zheng J, Gu C, Tong Y, et al., 2016, A Smart Superhydrophobic Coating on AZ31B Magnesium Alloy with Self-Healing Effect. *Advanced Materials Interfaces*, 3(14): 1500694.
- [17] Zhu M, Zuo W, Yu H, et al., 2006, Superhydrophobic Surface Directly Created by Electrospinning based on Hydrophilic Material. *Journal of Materials Science*, 41(12): 3793–3797.

**Publisher's note**

Bio-Byword Scientific Publishing remains neutral with regard to jurisdictional claims in published maps and institutional affiliations.